

Delving Deep into Semantic Relation Distillation

Zhaoyi Yan, Kangjun Liu, Qixiang Ye

Abstract—Knowledge distillation has become a cornerstone technique in deep learning, facilitating the transfer of knowledge from complex models to lightweight counterparts. Traditional distillation approaches focus on transferring knowledge at the instance level, but fail to capture nuanced semantic relationships within the data. In response, this paper introduces a novel methodology, **Semantics-based Relation Knowledge Distillation (SeRKD)**, which reimagines knowledge distillation through a semantics-relation lens among each sample. By leveraging semantic components, *i.e.*, superpixels, SeRKD enables a more comprehensive and context-aware transfer of knowledge, which skillfully integrates superpixel-based semantic extraction with relation-based knowledge distillation for a sophisticated model compression and distillation. Particularly, the proposed method is naturally relevant in the domain of Vision Transformers (ViTs), where visual tokens serve as fundamental units of representation. Experimental evaluations on benchmark datasets demonstrate the superiority of SeRKD over existing methods, underscoring its efficacy in enhancing model performance and generalization capabilities.

Index Terms—Vision Transformer, Superpixel, Relation-based Knowledge Distillation, Knowledge Distillation.

I. INTRODUCTION

In the past decade, knowledge distillation [1] has become a cornerstone technique in deep learning, especially in scenarios where deploying large-scale models is impractical due to computational constraints or deployment considerations. This method enables the transfer of knowledge from complex, computationally expensive models, referred to as “teacher” models, to more lightweight “student” models. Its applications span various domains, including computer vision [2], natural language processing [3], and speech recognition [4], where model efficiency and scalability are paramount.

Traditionally, knowledge distillation methods have always focused predominantly on transferring information at the instance level. These methods can be categorized into logit-based approaches [5]–[9] and feature-based approaches [10]–[14], which aim to match the output probabilities or intermediate representations between teacher and student models. Additionally, relation-based approaches [15], [16] have gained attention for capturing complex dependencies and intrinsic knowledge by modeling relationships or correlations between different instances or categories.

However, these methods often fail to capture the intricate semantic relationships inherent in the data. This limitation

has spurred research into methodologies that leverage semantic understanding and contextual information to enhance the distillation process. Meanwhile, recent advancements [17], [18] underscore the necessity of moving beyond instance-level knowledge transfer, emphasizing the importance of capturing and transferring more nuanced and contextually relevant information. This shift is particularly crucial given the increasing availability of large-scale datasets and the development of sophisticated model architectures.

Inspired by these observations, we propose a novel method called **Semantics-based Relation Knowledge Distillation (SeRKD)**. This approach leverages superpixels [19], [20] to extract semantic components, facilitating a more comprehensive and context-aware transfer of knowledge. By combining superpixel-based semantic extraction with relation-based knowledge distillation, SeRKD offers a sophisticated and nuanced approach to model compression and distillation. Our methodology reimagines knowledge distillation from a semantics-centric perspective, providing more effective knowledge transfer compared to conventional instance-level methods. Building upon the foundational work of Hinton et al. [1], our approach goes beyond simply matching output probabilities or intermediate representations by incorporating semantic relationships within the data.

As illustrated in Figure 1, our approach differs from traditional relation-based distillation techniques by focusing on semantic-superpixel tokens at the instance level. The core of our methodology lies in the extraction and utilization of semantic relationships within the data, capturing relationships between different semantic components to enrich the distillation process with valuable contextual insights. This semantics-centric approach enables a more comprehensive and contextually aware transfer of knowledge, leading to improved model performance and generalization capabilities.

Our methodology is particularly well-suited for Vision Transformers (ViTs), which rely on visual tokens as fundamental units of representation. Aligned with the token-based architecture of ViTs, our method ensures seamless integration and enhances performance. By extracting knowledge from semantic parts represented by superpixels, our approach provides a fine-grained understanding of image content. This detailed semantic extraction significantly boosts the efficiency and accuracy of the distillation process.

The contributions of this study are as follows:

- We introduce a semantics-centric approach to knowledge distillation, providing a deeper and more nuanced understanding of data and enabling more effective knowledge transfer compared to conventional instance-level methods.
- Technically, our proposed framework, **Semantics-based Relation Knowledge Distillation (SeRKD)**, combines superpixel extraction with relation-based knowledge dis-

Q. Ye is with the School of Electronic, Electrical and Communication Engineering, University of Chinese Academy of Sciences, Beijing, China and also with Peng Cheng Laboratory, Shenzhen, China (e-mail: qxye@ucas.ac.cn).

Z. Yan is with School of with the School of Computer Science and Technology, Harbin Institute of Technology, Harbin 150001, China (e-mail: yanzhaoyi@outlook.com).

K. Liu is with Peng Cheng Laboratory, Shenzhen, China (e-mail: liukj@pcl.ac.cn).

Corresponding Author: Qixiang Ye.

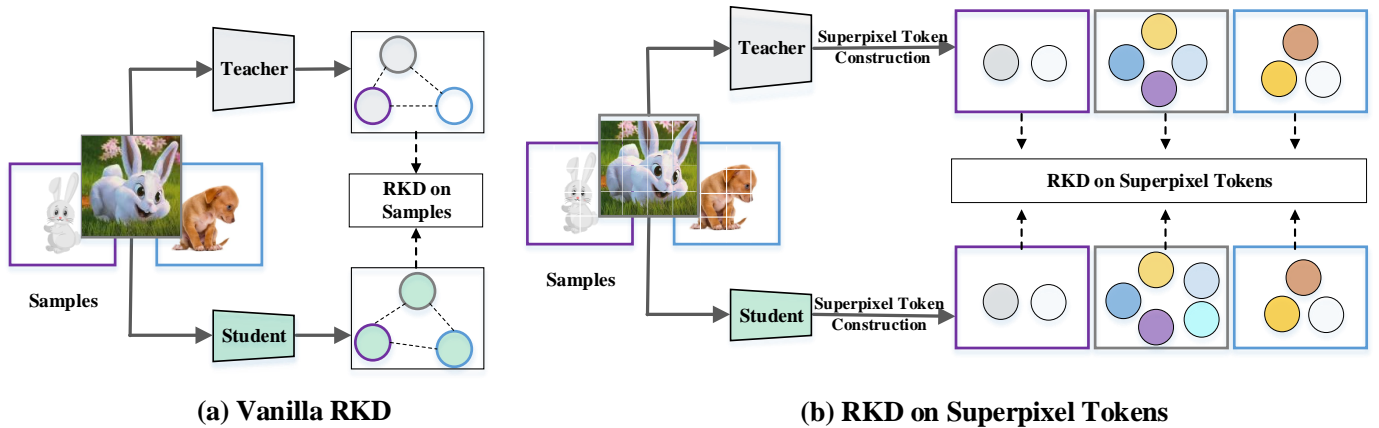


Fig. 1. Comparison of different relation-based distillation techniques. While vanilla RKD focuses on building relationships among samples, our method distills relational knowledge among semantic-superpixel tokens at an instance level.

tillation, offering a sophisticated and contextually rich approach to model compression and distillation.

- Experimental evaluations conducted on various benchmark datasets demonstrate the superior performance of SeRKD over existing methods, highlighting its efficacy in enhancing model performance and generalization capabilities.

In summary, this paper presents a novel approach to knowledge distillation that transcends the limitations of traditional methods by embracing a semantics-centric perspective and integrating recent advancements in superpixel-based segmentation techniques. By enriching the distillation process with semantic understanding and contextual information, our methodology opens new avenues for more effective and contextually rich knowledge transfer in machine learning models.

II. RELATED WORK

In this section, we firstly briefly review some recent works regarding knowledge distillation. Secondly, existing works about superpixel methods in model training are investigated.

A. Knowledge Distillation

Knowledge distillation, originating from the seminal work of Hinton et al. [1], has evolved as a fundamental methodology for model training and compression. Numerous related works [6]–[8], [21] have subsequently emerged, focusing on utilizing the teacher’s predictions as “soft” labels to guide and supervise students. Beyond such logit-based methods, this avenue expands with various works [10], [12], [13], delving into diverse perspectives of distilling feature-based knowledge, which usually transfer the spatial-wise knowledge in teacher model’s intermediate features for adequate representation learning in student model.

One of the pivotal advancements in knowledge distillation is the introduction of Relation Knowledge Distillation (RKD) [15]. RKD stands out as a significant contribution, particularly for its emphasis on correlation learning within the same batch from one model to another. The method effectively captures nuanced relationships between data samples, contributing to

improved knowledge transfer, which motivates us to explore further about the semantic correlation distillation.

However, a prevailing trend in the literature is the dominance of methods designed for CNNs, with limited applicability to prevalent transformer-based models [22]. Notably, the Vision Transformer (ViT) series [23] has gained prominence as the most widely used network architecture. The scarcity of methods suitable for transformer-based models motivates the exploration of novel techniques that can cater to the evolving landscape of modern deep learning architectures. To contribute to the Vision Transformer (ViT) community through Knowledge Distillation (KD), DeiT [24] firstly suggests distilling knowledge from CNNs to Vision Transformers. Subsequently, DearKD [25] introduces a dual-stage learning framework, where knowledge distillation occurs exclusively from the intermediate features of CNNs during the initial stage. CSKD [26] employs a technique to distill spatial-wise knowledge to all patch tokens of ViT directly from the corresponding spatial responses of CNNs, eliminating the need for utilizing any intermediate features. Recently, G2SD [27] enables effective bidirectional distillation between CNNs and ViTs through a generic-to-specific framework that transfers both task-agnostic and task-specific knowledge. Those previous works prove the potential of distilling knowledge from CNNs to Vision Transformers, but lacking the exploration concerning the semantic distillation from well-learned Vision Transformers.

In departure from previous knowledge distillation methods, we propose the Semantics-based Relation Knowledge Distillation (SeRKD) algorithm. Distinguished by its part-wise correlation learning approach, SeRKD is uniquely positioned to enhance knowledge transfer learning for a diverse array of transformer-based architectures, including the widely adopted ViT series, while also accommodating CNN-based models. The versatility of SeRKD makes it a valuable contribution, addressing the limitations of existing methods and opening new avenues for effective knowledge distillation across various deep learning architectures.

B. Superpixel Methods

Superpixel algorithms are fundamentally categorized into graph-based and clustering-based methods. Graph-based methods conceptualize image pixels as nodes within a graph structure, segmenting these nodes based on the connectivity of adjacent pixel edges, as detailed in seminal works by [28]–[30]. Conversely, clustering-based methods employ established clustering techniques like k -means to form superpixels, utilizing diverse feature representations to enhance the granularity of segmentation, as explored by [31], [32]. ETPS [33] and SEEDS [34] initially partition the image into regular grids and utilize different energy functions to optimize the exchange of pixels between neighboring superpixels.

The advent of deep learning has precipitated a shift towards more sophisticated deep clustering approaches, as evidenced by the literature [35]–[38]. These methods seek to harness deep feature representations to augment the efficiency and accuracy of superpixel generation. Notably, SEAL [39] integrates deep learning features with traditional superpixel algorithms for enhanced feature learning. Similarly, SSN [19] introduces an innovative end-to-end differentiable superpixel segmentation framework. Followed by SSN, SPIN [40] introduces Intra-Superpixel Attention (ISPA) and Superpixel Cross Attention (SPCA) modules in ViTs for super-resolution tasks. Similarly, STViT [20] proposes a super token sampling algorithm to further refine the efficiency and effectiveness of superpixel segmentation.

In this paper, we construct relation structures for knowledge distillation using semantic parts derived from superpixel algorithms. Leveraging advanced methods like SSN [19], SPIN [40], or STViT [20], we enhance the distillation process through meaningful image segmentation. This approach captures semantic relationships within the data, facilitating more effective knowledge transfer and improving performance across CNNs and Vision Transformers.

III. PRELIMINARY

A. Relation-based Knowledge Distillation

Relation-based knowledge distillation aims to encapsulate the relational dynamics between training examples in the feature/output representation space. Such relation-based knowledge can capture the structure information in the data embedding space [15], [16], [41]–[43]. Park *et al.* [15] exploit the distance-wise metric \mathcal{L}_{RD} and angle-wise metric \mathcal{L}_{RA} among training samples in the batch. \mathcal{L}_{RD} is defined over pairs of examples and is concerned with the Euclidean distances in the representation space. For a pair of examples, the distance-wise potential $\psi_D(u_i, u_j)$ is the normalized Euclidean distance between them:

$$\psi_D(u_i, u_j) = \frac{1}{\nu} \|u_i - u_j\|_2, \quad (1)$$

where ν is the normalization factor and u_i is the output representation of the student/teacher network. The loss, \mathcal{L}_{RD} , then minimizes the Huber loss l_δ between the student's and

teacher's distance-wise potentials, fostering a similar relational structure in the student. Huber loss l_δ is formulated as:

$$l_\delta = \begin{cases} \frac{1}{2}(x - y)^2 & \text{for } |x - y| \leq 1, \\ |x - y| - \frac{1}{2}, & \text{otherwise.} \end{cases} \quad (2)$$

Angle-wise Distillation Loss (\mathcal{L}_{RA}) focuses on the angles formed by triplets of examples, capturing higher-order relational information. The angle-wise potential $\psi_A(u_i, u_j, u_k)$ is the cosine of the angle formed by three data points:

$$\psi_A(u_i, u_j, u_k) = \langle e^{ij}, e^{kj} \rangle, \quad (3)$$

where e^{ij} and e^{kj} are unit vectors. The corresponding loss, \mathcal{L}_{RA} , minimizes the Huber loss between the teacher's and student's angle-wise potentials.

Training with RKD involves combining these relational losses with a task-specific loss (\mathcal{L}_{task}). The holistic objective is thus:

$$\mathcal{L}_{Total} = \mathcal{L}_{task} + \lambda_D \mathcal{L}_{RD} + \lambda_A \mathcal{L}_{RA}, \quad (4)$$

where λ_D and λ_A are the weights of the losses and all possible pairs and triplets from a given mini-batch are utilized for distillation.

These relational losses facilitate a more nuanced transfer of knowledge, focusing not just on direct outputs but also on the intricate geometric relationships between them, promising a richer and more flexible learning experience for the student model.

B. Transformer Representations

The Vision Transformer (ViT [23]) framework transforms an input image into a structured sequence of vector representations, treating the image as a series of discrete 'words' or patches. For a given image $I \in \mathcal{R}^{H \times W \times C}$, it is systematically segmented into $N = \frac{H \times W}{P^2}$ distinct patches $\{I_i^p\}_{i=1}^N$, with H , W , C , and P denoting the height, width, number of channels, and patch dimension, respectively. Each patch I_i^p represents a flattened vector of dimension $N \times (P^2 C)$. This approach is demonstrated using a typical image size of $224 \times 224 \times 3$, which is segmented into a 14×14 patch grid, with each patch measuring $16 \times 16 \times 3$. Embedded positional encodings enhance the spatial relevance of these patches. Subsequent processing through the Transformer's architecture, which includes layers of multi-head self-attention [44] and feed-forward networks, refines these vectors into advanced image representations.

C. Superpixel Sampling Networks

Superpixel Sampling Networks (SSN [19]) introduced a differentiable approach for generating superpixels. Let F_i represent the feature value at pixel i and S_j denote superpixel j . The process begins by initializing superpixel centers using averaged features within regular grid cells, typically a 3×3 grid. Superpixels are refined iteratively by updating the association between pixels and superpixels using a Radial Basis Function (RBF) kernel. The association matrix at iteration t , denoted as $Q^t \in \mathcal{R}^{n \times m}$, where n is the total number of

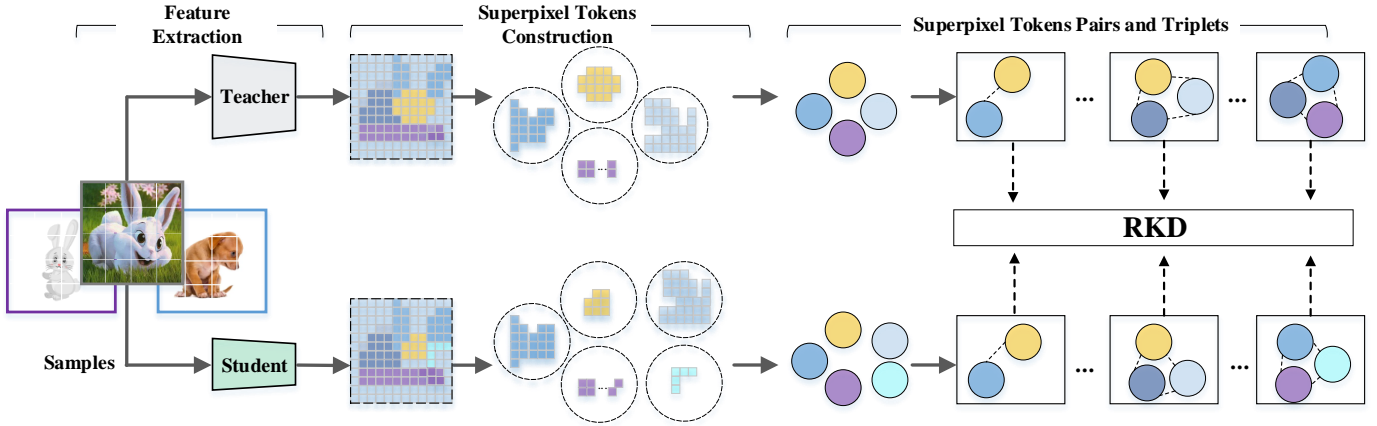


Fig. 2. Illustration of the proposed SeRKD method, which mainly contains the mechanism of the feature extraction, the construction of semantic superpixel tokens, and the alignment of relation knowledge upon the superpixel tokens.

spatial pixels and m is the number of superpixels, is updated as follows:

$$Q_{ij}^t = \exp(-\|\mathbf{F}_i - S_j^{t-1}\|^2), \quad (5)$$

reflecting the association based on the squared Euclidean distance between the feature of each pixel and the superpixel center from the previous iteration ($t-1$).

To enhance computational efficiency, SSN restricts the computation of associations to the 9 nearest neighboring pixels. The superpixel centers are then updated in each iteration by aggregating the associated features:

$$S_j^t = \frac{1}{Z_j^t} \sum_i Q_{ij}^t \mathbf{F}_i, \quad (6)$$

where S_j^t denotes the updated superpixel center at current iteration t and $Z_j^t = \sum_i Q_{ij}^t$.

IV. THE PROPOSED METHOD

A. Building Superpixel Tokens

1) *Building Superpixel Tokens for ViTs*: Given an input image $I \in \mathcal{R}^{H \times W \times C}$, it is initially processed by the ViT to transform the image into a sequence of patch tokens $\{T_i\}_{i=1}^N$, where each token T_i corresponds to a patch I_i^p processed by the multiple transformer blocks. To integrate superpixels into the ViT framework, we need to build superpixel tokens from the existing patch tokens. Following [20], we adopt a more attention-like manner to compute the association map:

$$Q^t = \text{Softmax}\left(\frac{\mathbf{T} S^{t-1T}}{\sqrt{d}}\right), \quad (7)$$

where d denotes the dimensionality C of the token representations. The superpixel token S^t at iteration t is computed as follows:

$$S^t = (\hat{Q}^t)^T \mathbf{T}, \quad (8)$$

where \hat{Q}^t is the column-normalized Q^t . Similar to [19], [20], to reduce computation burden, for each token, we restrict the corresponding local 3×3 surrounding superpixel tokens. S^0 is obtained by performing an average pooling with grid size $H_t \times W_t$ on \mathbf{T} . The stride remains the same as the grid size.

2) *Building Superpixel Tokens on CNNs*: Given we only build the associations around its 9 surrounding tokens due to the large computation burden of building the associations for all the tokens, we refine the superpixel tokens with a tiny learnable network Φ . For CNN features, which lack the structured patch tokens of Vision Transformers (ViTs), we propose a tokenization strategy to segment the CNN feature map into discrete tokens. Given the feature map \mathbf{F} , we define the tokenization operation as:

$$\mathbf{P} = \text{Tokenize}(\mathbf{F}, \Theta, H_p, W_p), \quad (9)$$

where $\mathbf{P} \in \mathcal{R}^{L \times C}$ is the matrix of tokens, $L = \frac{H \times W}{H_p \times W_p}$ is the number of tokens, and H_p, W_p are the dimensions of the tokenizing window. The parameter set Θ defines the tokenizer's rules, which can be parameter-free (e.g., max-pooling, average-pooling) or parameterized (e.g., strided-convolution). This tokenization method enables the construction of superpixel tokens from CNN features, facilitating enhanced image representation analogous to ViTs.

B. Relation Knowledge Distillation on Superpixel Tokens

Traditionally, the application of Relation-based Knowledge Distillation (RKD) in Vision Transformers (ViTs) has not been explicitly explored, particularly with respect to the direct use of raw token representations. Recognizing this gap, we initially experimented with RKD on raw ViT tokens. However, these preliminary attempts highlighted a significant performance degradation compared with the traditional KD [1] method, suggesting the inadequacy of direct RKD application on raw tokens within the ViT framework. To address this challenge, we introduce a novel approach that firstly constructs semantic superpixel tokens as described in IV-A. Subsequently, RKD is applied to these superpixel tokens, thereby aligning the distillation process more closely with the inherent structure and semantic layout of the data.

1) *Semantic Enhancement through Superpixel Tokens*: In this paper, we pivot from conventional instance-based relational learning to a more semantically grounded methodology. Utilizing superpixel tokens, detailed in Section IV-A, we enrich the visual tokens with semantic coherence. This semantic

enrichment forms the foundation for our adapted RKD process. We use \mathbf{S} to represent the set of superpixel tokens derived from the visual tokens \mathbf{T} via the superpixel clustering method described in Section IV-A.

2) *Semantics-based RKD Loss*: Building on these semantically enriched tokens, we recalibrate the RKD loss to operate in this new semantic token space. The distance-wise and angle-wise components of RKD loss are redefined to reflect the semantic relationships within the superpixel tokens. The revised RKD losses for pairs and triplets of superpixel tokens are formulated as follows:

$$\mathcal{L}_{\text{RD}}^{\text{SP}} = \frac{1}{\nu'} \sum_{i,j} l_{\delta}(\psi_{\text{D}}(s_i, s_j), \psi_{\text{D}}(s'_i, s'_j)), \quad (10)$$

$$\mathcal{L}_{\text{RA}}^{\text{SP}} = \sum_{i,j,k} l_{\delta}(\psi_{\text{A}}(s_i, s_j, s_k), \psi_{\text{A}}(s'_i, s'_j, s'_k)), \quad (11)$$

where s_i, s_j, s_k represent the superpixel tokens for the student model, s'_i, s'_j, s'_k are for the teacher model, and ν' is a normalization factor for the superpixel-based RKD.

3) *Semantic-focused RKD*: Our method emphasizes the crucial role of semantics in building relational knowledge. By focusing on semantic construction prior to distillation, the model internalizes more meaningful and contextually relevant relationships.

Similar to RKD [15] adopted in classification task, Knowledge distillation loss \mathcal{L}_{KD} [1] and cross-entropy classification loss \mathcal{L}_{cls} are also used, resulting the final distillation loss \mathcal{L}_{dis} :

$$\mathcal{L}_{\text{dis}} = \mathcal{L}_{\text{cls}} + \lambda_K \mathcal{L}_{\text{KD}} + \lambda_F \mathcal{L}_F + \lambda_D \mathcal{L}_{\text{RD}}^{\text{SP}} + \lambda_A \mathcal{L}_{\text{RA}}^{\text{SP}}, \quad (12)$$

where $\lambda_K, \lambda_F, \lambda_D$ and λ_A are the hyper-parameters to balance the losses. \mathcal{L}_F is defined as the \mathcal{L}_2 loss between student feature F_s and teacher feature F_t . \mathcal{L}_{KD} is derived from [1] formulated as:

$$\sum_{I_i} \text{KL}\left(\text{softmax}\left(\frac{l_t(I_i)}{\tau}\right), \text{softmax}\left(\frac{l_s(I_i)}{\tau}\right)\right), \quad (13)$$

where $l_t(I_i)/l_s(I_i)$ denotes the logits (pre-softmax activation outputs) of the teacher/student model for a given input image I_i . τ is used to control the smoothness of the output probability distribution obtained from the softmax function applied to the logits.

V. EXPERIMENTAL ANALYSIS

This section presents a comprehensive experimental evaluation of our proposed Semantics-based Relation Knowledge Distillation (SeRKD). We primarily focus on the ImageNet-1k dataset [45] to assess SeRKD’s effectiveness. Additionally, we extend our experiments to transfer learning tasks, demonstrating SeRKD’s robust generalization capabilities. Ablation studies and detailed visualizations are also provided for a deeper understanding of the method. $T = 1, \lambda_K = 1, \lambda_F = 1, \lambda_D = 0.5$ and $\lambda_A = 1$ by default.

A. Implementation Details

Our experiments utilize an MAE-base [46] as the teacher, attaining a top-1 accuracy of 83.6% on ImageNet-1k. Each model undergoes training for 300 epochs using a batch size of 1024, trained on 8 NVIDIA V100 GPUs, *i.e.*, 128 images per GPU. We employ the AdamW optimizer with an initial learning rate of 0.001, employing a cosine decay learning rate schedule. The weight decay parameter is set to 0.05. For input images, we use a resolution of 224×224 . Our data augmentation strategy includes Mixup, Cutmix, and RandAugment. Following DeiT [24], an additional distillation token is employed in a similar fashion to the class token for the student network. For classification on ImageNet, the total number of tokens is $14 \times 14 + 1 + 1 = 198$. Apart from the conventional classification head applied to the class token, a distillation head is also applied to the distillation token. We calculate the average value of the logits produced by the classification head and the distillation head to obtain the final prediction. For \mathcal{L}_{KD} , it is applied to the logits produced by the distillation head.

We use the visual tokens (with the class token and distillation token removed) from the final transformer block to perform superpixel clustering and relation knowledge distillation. To this end, \mathcal{L}_F is applied to these visual tokens. These visual tokens are further used to perform superpixel clustering for relation distillation. H_t and W_t are both set to 2, indicating that the initial superpixels S^0 are obtained by performing average pooling on the visual tokens. Therefore, the superpixel size is $14/2 \times 14/2 = 7 \times 7$. We set the iteration $T = 1$ by default, as we find that more iterations do not yield better performance.

We train variants of our SeRKD model: SeRKD-Ti (SeRKD-Tiny), SeRKD-S (SeRKD-Small), the student architecture is the same as DeiT [24].

B. Implementation and Complexity of RKD Loss on Superpixel Tokens

Here are the implementations of the angle-wise and distance-wise loss functions for relation-based knowledge distillation in Vision Transformers. `RkdDistance_token` and `RkdAngle_token` are the functions of $\mathcal{L}_{\text{RD}}^{\text{SP}}$ and $\mathcal{L}_{\text{RA}}^{\text{SP}}$, respectively.

```
def extended_rkdangle(vit_feat):
    B, L, C = vit_feat.shape
    # Compute pairwise differences
    diff = vit_feat.unsqueeze(2) - vit_feat.
    unsqueeze(1) # Shape: [B, L, L, C]
    norm_diff = F.normalize(diff, p=2, dim=3) #
    Shape: [B, L, L, C]
    # Reshape for batch matrix multiplication
    norm_diff_flat = norm_diff.view(B * L, L, C)
    # Perform batch matrix multiplication to get the
    angle potentials
    angle_flat = torch.bmm(norm_diff_flat,
    norm_diff_flat.transpose(1, 2))
    # Reshape back to original dimensions
    angle = angle_flat.view(B, L, L, L)
    return angle
class RkdAngle_token(nn.Module):
    def forward(self, student, teacher):
        with torch.no_grad():
            t_angle = extended_rkdangle(teacher).
            view(-1)
```

```

        s_angle = extended_rkdangle(student).view
        (-1)
        loss = F.smooth_l1_loss(s_angle, t_angle,
        reduction='mean')
        return loss
def batch_pdist(e, squared=False, eps=1e-12):
    e_square = e.pow(2).sum(dim=2)
    prod = torch.einsum('bik,bjk->bij', e, e) #
    Pairwise dot products
    res = (e_square.unsqueeze(2) + e_square.
    unsqueeze(1) - 2 * prod).clamp(min=eps)
    if not squared:
        res = res.sqrt().clone()
    # Set the diagonal to zero across all batches
    res[:, torch.arange(res.size(1)), torch.arange(
    res.size(2))] = 0
    return res
class RkdDistance_token(nn.Module):
    def forward(self, student, teacher):
        L = student.shape[1]
        with torch.no_grad():
            t_d = batch_pdist(teacher, squared=False)
        ) # Shape: [B, L, L]
            mean_td = t_d.sum(dim=(1, 2), keepdim=
            True) / (L * (L - 1)) # Normalize
            t_d = t_d / mean_td
            d = batch_pdist(student, squared=False) #
            Shape: [B, L, L]
            mean_d = d.sum(dim=(1, 2), keepdim=True) / (
            L * (L - 1)) # Normalize
            d = d / mean_d
            loss = F.smooth_l1_loss(d, t_d, reduction='
            mean')
        return loss
loss_distill_angle = RkdAngle_token()
loss_distill_rkd_dist = RkdDistance_token()
loss_rkd_angle = args.angle_w * loss_distill_angle(
    stu_super_tokens, tec_super_tokens.detach())
loss_rkd_dist = args.dist_w * loss_distill_rkd_dist(
    stu_super_tokens, tec_super_tokens.detach())

```

Given an input superpixel tensor with shape (B, L, C) , where B is the batch size, L is the number of superpixel tokens, and C is the feature dimension, the complexity analysis is as follows:

a) *Complexity Analysis of RkdAngle_token:*

Time Complexity:

- Pairwise Difference Computation: $\mathcal{O}(BL^2C)$
- Normalization: $\mathcal{O}(BL^2C)$
- Batch Matrix Multiplication: $\mathcal{O}(BL^2C)$
- Reshaping: $\mathcal{O}(1)$ (negligible)

Overall, the time complexity is $\mathcal{O}(BL^2C)$.

Space Complexity:

- Intermediate Tensors: $\mathcal{O}(BL^2C)$ each
- Angle Tensor: $\mathcal{O}(BL^3)$

Overall, the space complexity is $\mathcal{O}(BL^3)$.

b) *Complexity Analysis of RkdDistance_token:*

Time Complexity:

- Pairwise Distance Computation: $\mathcal{O}(BL^2C)$
- Normalization: $\mathcal{O}(BL^2)$
- Loss Calculation: $\mathcal{O}(BL^2)$

Overall, the time complexity is $\mathcal{O}(BL^2C)$.

Space Complexity:

- Pairwise Distance Tensor: $\mathcal{O}(BL^2)$

Overall, the space complexity is $\mathcal{O}(BL^2)$.

Remark: From the analysis above, it is evident that the primary space complexity arises from the `RkdAngle_token` function. For instance, with float16 precision, the memory consumption of `RkdAngle_token` is approximately 0.95 GB for $B = 128$, $L = 49$, and $C = 768$. However, when L increases to $14 \times 14 = 196$, the memory usage escalates to 17.73 GB, leading to the risk of out-of-memory (OOM) errors. Therefore, for our setting, we recommend using $H_t = W_t = 2$ to ensure the number of superpixel tokens is 49, making the computation and space complexity more manageable.

C. Performance on ImageNet-1k

We evaluate SeRKD on the ImageNet-1k [45] dataset, a prominent large-scale image classification benchmark with 1.28 million training images and 50,000 validation images across 1,000 categories. ImageNet-1k offers a challenging environment to test the efficacy of our SeRKD approach.

1) *ImageNet classification on SeRKD-ViT:* The results in Table II highlight SeRKD’s superior performance on ImageNet-1k.

TABLE I
RESULTS ON IMAGENET-1K. * MEANS THAT REGNETS ARE OPTIMIZED WITH SIMILAR OPTIMIZATION PROCEDURES AS DEiT, SERVING AS TEACHERS FOR DEiT AND OUR CSKD. “VAL-REAL” REPRESENTS THE RESULTS OF THE IMAGENET REAL VALIDATION SET.

Method	#params(M)	image size	val
<i>CNNs</i>			
ResNet18 [47]	12M	224 ²	69.8
ResNet50 [47]	25M	224 ²	76.2
ResNet101 [47]	45M	224 ²	77.4
ResNet152 [47]	60M	224 ²	78.3
RegNetY-4GF [48]	21M	224 ²	80.0
RegNetY-8GF [48]	39M	224 ²	81.7
RegNetY-16GF [48]	84M	224 ²	82.9
EffiNet-B0 [49]	5M	224 ²	77.1
EffiNet-B3 [49]	12M	224 ²	81.6
<i>VITs</i>			
ViT-B/16 [23]	86M	384 ²	77.9
ViT-L/16 [23]	307M	384 ²	76.5
DeiT-Ti [24]	6M	224 ²	74.5
DeiT-S [24]	22M	224 ²	81.2
DearKD-Ti [25]	5M	224 ²	74.8
DearKD-S [25]	22M	224 ²	81.5
CSKD-Ti [26]	6M	224 ²	76.3
CSKD-S [26]	22M	224 ²	82.3
SeRKD-Ti	6M	224 ²	76.8
SeRKD-S	22M	224 ²	82.5

2) *ImageNet Classification on CNN:* Implementing SeRKD on CNN architectures necessitates the tokenization of CNN features, adapting them for relational knowledge distillation. We investigate different tokenization methods to determine the optimal approach for distilling knowledge from ResNet-101 to ResNet-18.

We adopt the feature maps of the first three stages for knowledge distillation. For the 1-st, 2-nd, and 3-rd stages, we perform pooling or stride convolution with stride=4, 2, 1, respectively. The number of image tokens of each stage is

kept at $14 \times 14 = 196$. Both student and teacher models share the same tokenizer setup to ensure compatible feature representation. Notably, for parameterized tokenizers like strided convolutions, teacher gradients are detached to ease the learning of the student and the tokenizer.

TABLE II
PERFORMANCE OF DIFFERENT TOKENIZATION METHODS FOR STUDENT RESNET-18 WITH TEACHER RESNET-101 ON IMAGENET-1K.

Method	Tokenizer	Top-1 Accuracy (%)
KD [1]	-	71.09
RKD [15]	-	71.82
SeRKD	Max Pooling	70.61
	Average Pooling	72.22
	Strided Convolutions	72.25

Strided convolutions and average pooling deliver the top two performances with only marginal differences, underscoring their effectiveness in preserving spatial hierarchies crucial for detailed feature transfer. However, max pooling shows slightly reduced efficacy, likely due to its potential for detail loss. When employing average pooling or strided convolutions as tokenizers, our SeRKD method notably surpasses traditional KD and RKD, achieving significant performance gains.

D. Transfer Learning to Downstream Datasets

We conduct experiments to evaluate the effectiveness of our proposed method in the context of transfer learning to various downstream datasets. The datasets used for these experiments include CIFAR10 [50], CIFAR100 [50] and Cars [51]. Detailed information about each dataset is presented in Table III.

Our experimental results are summarized in Table IV. As can be observed, our proposed method, denoted as SeRKD, achieves significantly superior transfer learning performances compared to the DeiT and DearKD approaches across all considered downstream datasets. Specifically, our method SeRKD-S surpasses CSKD-S by 0.1%, 1.0%, and 0.4% over CIFAR10, CIFAR100, and Cars.

TABLE III
DOWNSTREAM DATASET INFORMATION FOR TRANSFER LEARNING.

dataset	training size	val size	#classes
CIFAR10	50,000	10,000	10
CIFAR100	50,000	10,000	100
Stanford Cars	8,144	8,041	196

TABLE IV
TRANSFER PERFORMANCE IN DOWNSTREAM TASKS. * REPRESENTS THAT THE RESULTS ARE BASED ON OUR IMPLEMENTATION.

	CIFAR10	CIFAR100	Cars
DeiT-Ti*	98.1	86.1	92.1
DearKD-Ti	97.5	85.7	89.0
CSKD-Ti	98.5	87.0	93.1
SeRKD-Ti	98.6	87.8	93.6
DeiT-S*	98.7	89.2	91.7
DearKD-S	98.4	89.3	91.3
CSKD-S	99.1	90.3	93.7
SeRKD-S	99.2	91.3	94.1

VI. ABLATION STUDY

A. Ablations on the Key Components of SeRKD

To understand the contributions of different components of our proposed SeRKD framework, we conduct a series of ablation experiments. The results in Table V demonstrate the effectiveness of each component within the SeRKD framework. Specifically, we observe the following: The results in Table V demonstrate the effectiveness of each component within the SeRKD framework. Knowledge Distillation (KD) [1] method achieves an accuracy of 74.1%. By incorporating the feature-based loss \mathcal{L}_F , FitNet [52] shows a marginal improvement with an accuracy of 74.2%. Secondly, introducing superpixel-based clustering along with feature-based and distance-wise relational losses (\mathcal{L}_F and \mathcal{L}_{RD}^{SP}), SeRKD-Ti† significantly boosts the accuracy to 76.5%. When angle-wise relational loss (\mathcal{L}_{RA}^{SP}) is used in conjunction with superpixel clustering and distance-wise relational loss, the performance slightly decreases to 76.2%, highlighting the critical balance between these components. Finally, the full SeRKD-Ti model, integrating superpixel clustering with all relational and feature-based losses (\mathcal{L}_F , \mathcal{L}_{RD}^{SP} , and \mathcal{L}_{RA}^{SP}), achieves the highest accuracy of 76.8%, underscoring the complementary nature of these components. These ablation studies illustrate the importance of each component in enhancing the distillation process, validating our design choices for the SeRKD framework.

TABLE V
ABLATIONS ON THE KEY COMPONENTS OF SERKD.

Methods	Clustering	\mathcal{L}_F	\mathcal{L}_{RD}^{SP}	\mathcal{L}_{RA}^{SP}	Acc (%)
KD [1]					74.1
Fitnet [52]		✓			74.2
SeRKD-Ti†	Superpixel	✓	✓		76.5
SeRKD-Ti‡	Superpixel		✓	✓	76.2
SeRKD-Ti	Superpixel	✓	✓	✓	76.8

B. Ablation on Clustering Methods

In order to perform relation knowledge distillation on image tokens effectively, it is essential to first construct meaningful semantic representations. In this subsection, we explore three approaches for building semantics: direct-based, pooling-based (MaxPooling and AvgPooling), and superpixel-based.

The direct-based approach involves applying relation knowledge distillation directly on the image tokens without any prior semantic construction. Pooling-based methods aim to create semantics by aggregating tokens through pooling operations. The superpixel-based approach, which is ultimately adopted in our method, leverages the inherent semantic layout of the image to guide the token merging process. To establish a baseline for comparison, we remove the superpixel-based RKD loss from the training objective by setting $\lambda_D = \lambda_A = 0$.

The results presented in Table VI yield several key insights. When applying relation knowledge distillation directly on the image tokens, we observe a substantial performance degradation of 1.2% compared to the baseline setting. This significant

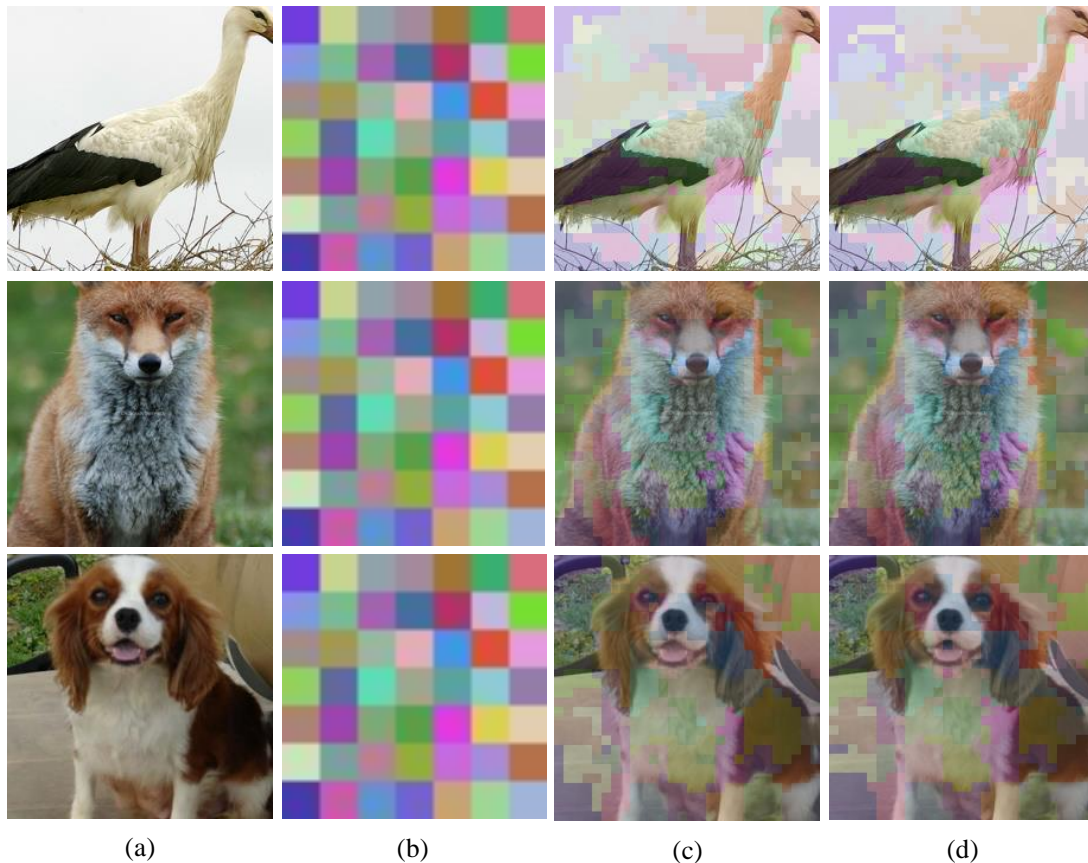


Fig. 3. Visualization of learned superpixel tokens in the SeRKD-S distillation setting. (a) is the input image, (b) is the superpixel map, (c) shows the superpixel tokens of the teacher, and (d) shows the learned superpixel tokens of the student.

drop in performance can be attributed to the large number of tokens (196) and the lack of essential semantic relations within individual tokens, hindering effective distillation. Employing pooling-based token merging methods leads to improved performance compared to the direct-based approach. However, the results still fall short of the baseline. This suggests that hard pooling methods alone are insufficient for capturing the complex semantic relationships inherent in image tokens.

In contrast, the superpixel-based token merging method, which respects the semantic layout of the image, surpasses the baseline approach, achieving a top-1 accuracy of 77.4%. This represents a notable improvement of 2.3% over the baseline, highlighting the effectiveness of leveraging semantic information in the token clustering process.

TABLE VI
PERFORMANCE OF SERKD-TI WITH DIFFERENT TOKEN MERGING METHODS. FOR THE DIRECT-BASED METHOD, WE REDUCE THE BATCH SIZE TO 32 PER GPU TO AVOID OOM.

Methods	Top-1 (%)	Top-5 (%)
Baseline	74.2	92.2
Direct-based	73.9	92.0
MaxPooling-based	73.3	91.5
AvgPooling-based	73.8	91.7
Superpixel-based	76.8	93.4

C. Visualization of Learned Superpixels

Figure 3 visualizes the superpixel tokens of the SeRKD-S distillation setting. In Figure 3(c), the superpixel tokens of the teacher MAE-base are shown, and Figure 3(d) displays the learned superpixel tokens of the student SeRKD-S. It is evident that these two types of superpixels share similar semantic regions, indicating that our RKD loss on these superpixel tokens effectively enhances the alignment of the semantic layout between the teacher and the student.

D. Ablation on Superpixel-RKD Loss

To investigate the impact of the Superpixel-RKD loss on the performance of SeRKD, we conduct an ablation study by varying the hyper-parameters λ_D and λ_A . Table VII presents the results of this study. Initially, we perform a search over different values of λ_K to establish a baseline model. Based on these preliminary experiments, we set $\lambda_K = 1$ for the baseline. Building upon this baseline, we explore the performance of SeRKD under various settings of λ_D and λ_A . The results, summarized in Table VII, demonstrate the impact of these hyper-parameters on the model's performance. After careful consideration of the results, we determine the optimal values of $\lambda_D = 0.5$ and $\lambda_A = 1$ for all our SeRKD training models. With these settings, SeRKD-Ti and SeRKD-S achieve top-1 accuracies of 76.8% and 82.5%, respectively, on the ImageNet dataset.

TABLE VII
PERFORMANCE OF SeRKD WITH DIFFERENT λ_K , λ_D , AND λ_A VALUES ON IMAGENET.

λ_K	λ_F	λ_D	λ_A	SeRKD-Ti	SeRKD-S
0.1	0	0	0	73.0	80.7
0.5	0	0	0	73.8	81.0
1	0	0	0	74.1	81.2
2	0	0	0	74.0	81.0
1	1	0	0	74.2	81.3
1	2	0	0	74.2	81.2
1	1	0.1	0.1	76.1	81.9
1	1	0.5	0.5	76.6	82.4
1	1	1.0	1.0	76.2	82.0
1	1	0.5	0.1	76.4	82.2
1	1	0.5	1.0	76.8	82.5
1	1	0.5	2.0	76.7	82.5

E. Ablation on Grid Size

We investigate the impact of grid sizes ($H_t \times W_t$) on the performance of SeRKD-Ti and SeRKD-S models. Table VIII presents the top-1 accuracy results with grid sizes of 1×1 , 2×2 , and 3×3 . For the 1×1 grid, the batch size was reduced to 32 per GPU to avoid OOM issues.

For the smallest grid size (1×1), the performance is lower (73.9% for SeRKD-Ti and 79.7% for SeRKD-S), likely due to the limited context each superpixel captures and the increased complexity, resulting in less effective relational knowledge distillation. The 2×2 grid size yields the highest accuracy (76.6% for SeRKD-Ti and 82.4% for SeRKD-S), suggesting it strikes a balance between capturing sufficient local context and maintaining computational efficiency. With the largest grid size (3×3), the performance decreases again (74.5% for SeRKD-Ti and 80.3% for SeRKD-S). This may be because the superpixels contain too large a context; in this case, a superpixel token aggregates a 48×48 region for a 224×224 image, making the relational knowledge less specific and effective.

In conclusion, the 2×2 grid size is optimal for the SeRKD method, providing a good trade-off between capturing local and global information and maintaining computational feasibility.

TABLE VIII
PERFORMANCE OF SeRKD-Ti/S WITH DIFFERENT GRID SIZE. FOR GRID SIZE 1×1 , WE REDUCE THE BATCH SIZE TO 32 PER GPU TO AVOID OOM.

Methods	$H_t \times W_t$	Top-1 (%)
SeRKD-Ti	1×1	73.9
SeRKD-S	1×1	79.7
SeRKD-Ti	2×2	76.6
SeRKD-S	2×2	82.4
SeRKD-Ti	3×3	74.5
SeRKD-S	3×3	80.3

F. Ablation on Iteration Times T

We conducted an ablation study to investigate the impact of the iteration count T on the performance of our SeRKD

models. We varied the number of iterations, specifically set at 1, 2, and 3, to understand its effect on the model’s top-1 accuracy. The results, summarized in Table VI, demonstrate the top-1 accuracy achieved by the SeRKD-Ti and SeRKD-S models at different iteration times. It is observed that for both Increasing SeRKD-Ti and SeRKD-S, the models perform best at $T = 1$, A further increase in iteration count marginal decreases the performances. The observed trend suggests that a higher number of iterations T does not necessarily contribute to better performance. This could be attributed to the potential over-smoothing of features, where repeated aggregation may dilute distinctive features that are crucial for accurate classification.

TABLE IX
PERFORMANCE OF SeRKD-Ti/S WITH DIFFERENT ITERATION TIMES T .

Methods	T	Top-1 (%)
SeRKD-Ti	1	76.8
SeRKD-S	1	82.5
SeRKD-Ti	2	76.6
SeRKD-S	2	82.4
SeRKD-Ti	3	76.2
SeRKD-S	3	82.1

VII. CONCLUSION

This paper introduced Semantics-based Relation Knowledge Distillation (SeRKD), a novel approach to knowledge distillation that leverages superpixels for semantic extraction and relation-based knowledge transfer. Our method demonstrated superior performance on benchmark datasets, particularly in the context of Vision Transformers (ViTs). SeRKD transcends traditional instance-level distillation techniques by incorporating semantic relationships, leading to enhanced model performance and generalization. This advancement not only offers superior efficiency in model compression but also opens new avenues for more nuanced and contextually rich knowledge transfer in various machine learning applications.

REFERENCES

- [1] G. Hinton, O. Vinyals, J. Dean *et al.*, “Distilling the knowledge in a neural network,” *arXiv preprint arXiv:1503.02531*, vol. 2, no. 7, 2015.
- [2] J. Gou, B. Yu, S. J. Maybank, and D. Tao, “Knowledge distillation: A survey,” *International Journal of Computer Vision*, vol. 129, no. 6, pp. 1789–1819, 2021.
- [3] S. Sun, Y. Cheng, Z. Gan, and J. Liu, “Patient knowledge distillation for bert model compression,” *arXiv preprint arXiv:1908.09355*, 2019.
- [4] J. W. Yoon, H. Lee, H. Y. Kim, W. I. Cho, and N. S. Kim, “Tutornet: Towards flexible knowledge distillation for end-to-end speech recognition,” *IEEE/ACM Transactions on Audio, Speech, and Language Processing*, vol. 29, pp. 1626–1638, 2021.
- [5] C. Li, G. Cheng, and J. Han, “Boosting knowledge distillation via intra-class logit distribution smoothing,” *IEEE Transactions on Circuits and Systems for Video Technology*, vol. 34, no. 6, pp. 4190–4201, 2024.
- [6] L. Beyer, X. Zhai, A. Royer, L. Markeeva, R. Anil, and A. Kolesnikov, “Knowledge distillation: A good teacher is patient and consistent,” in *CVPR*, 2022, pp. 10925–10934.
- [7] B. Zhao, Q. Cui, R. Song, Y. Qiu, and J. Liang, “Decoupled knowledge distillation,” in *CVPR*, 2022, pp. 11953–11962.
- [8] L. Yuan, F. E. Tay, G. Li, T. Wang, and J. Feng, “Revisiting knowledge distillation via label smoothing regularization,” in *CVPR*, 2020, pp. 3903–3911.

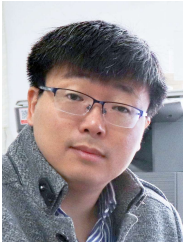
- [9] L. Xu, J. Ren, Z. Huang, W. Zheng, and Y. Chen, "Improving knowledge distillation via head and tail categories," *IEEE Transactions on Circuits and Systems for Video Technology*, vol. 34, no. 5, pp. 3465–3480, 2024.
- [10] A. Romero, N. Ballas, S. E. Kahou, A. Chassang, C. Gatta, and Y. Bengio, "Fitnets: Hints for thin deep nets," *CoRR*, vol. abs/1412.6550, 2015.
- [11] B. Heo, J. Kim, S. Yun, H. Park, N. Kwak, and J. Y. Choi, "A comprehensive overhaul of feature distillation," in *International Conference on Computer Vision*, 2019, pp. 1921–1930.
- [12] P. Chen, S. Liu, H. Zhao, and J. Jia, "Distilling knowledge via knowledge review," in *CVPR*, 2021, pp. 5008–5017.
- [13] J. Li, Z. Guo, H. Li, S. Han, J.-w. Baek, M. Yang, R. Yang, and S. Suh, "Rethinking feature-based knowledge distillation for face recognition," in *CVPR*, 2023, pp. 20156–20165.
- [14] K. Zhang, C. Zhang, S. Li, D. Zeng, and S. Ge, "Student network learning via evolutionary knowledge distillation," *IEEE Transactions on Circuits and Systems for Video Technology*, vol. 32, no. 4, pp. 2251–2263, 2021.
- [15] W. Park, D. Kim, Y. Lu, and M. Cho, "Relational knowledge distillation," in *CVPR*, 2019.
- [16] T. Huang, S. You, F. Wang, C. Qian, and C. Xu, "Knowledge distillation from a stronger teacher," *Conference on Neural Information Processing Systems*, vol. 35, pp. 33716–33727, 2022.
- [17] Y. Jin, J. Wang, and D. Lin, "Multi-level logit distillation," in *Proceedings of the IEEE/CVF Conference on Computer Vision and Pattern Recognition*, 2023, pp. 24276–24285.
- [18] S. Lin, H. Xie, B. Wang, K. Yu, X. Chang, X. Liang, and G. Wang, "Knowledge distillation via the target-aware transformer," in *Proceedings of the IEEE/CVF Conference on Computer Vision and Pattern Recognition*, 2022, pp. 10915–10924.
- [19] V. Jampani, D. Sun, M.-Y. Liu, M.-H. Yang, and J. Kautz, "Superpixel sampling networks," in *ECCV*, 2018, pp. 352–368.
- [20] H. Huang, X. Zhou, J. Cao, R. He, and T. Tan, "Vision transformer with super token sampling," in *Proceedings of the IEEE/CVF Conference on Computer Vision and Pattern Recognition*, 2023, pp. 22690–22699.
- [21] W. Zhang, Y. Guo, J. Wang, J. Zhu, and H. Zeng, "Collaborative knowledge distillation," *IEEE Transactions on Circuits and Systems for Video Technology*, vol. 34, no. 8, pp. 7601–7613, 2024.
- [22] A. Vaswani, N. Shazeer, N. Parmar, J. Uszkoreit, L. Jones, A. N. Gomez, L. Kaiser, and I. Polosukhin, "Attention is all you need," in *NeurIPS*, 2017.
- [23] A. Dosovitskiy, L. Beyer, A. Kolesnikov, D. Weissenborn, X. Zhai, T. Unterthiner, M. Dehghani, M. Minderer, G. Heigold, S. Gelly *et al.*, "An image is worth 16x16 words: Transformers for image recognition at scale," *preprint arXiv:2010.11929*, 2020.
- [24] H. Touvron, M. Cord, M. Douze, F. Massa, A. Sablayrolles, and H. Jégou, "Training data-efficient image transformers & distillation through attention," *preprint arXiv:2012.12877*, 2020.
- [25] X. Chen, Q. Cao, Y. Zhong, J. Zhang, S. Gao, and D. Tao, "Dearkd: data-efficient early knowledge distillation for vision transformers," in *CVPR*, 2022, pp. 12052–12062.
- [26] B. Zhao, R. Song, and J. Liang, "Cumulative spatial knowledge distillation for vision transformers," in *ICCV*, 2023, pp. 6146–6155.
- [27] W. Huang, Z. Peng, L. Dong, F. Wei, Q. Ye, and J. Jiao, "Generic-to-specific distillation of masked autoencoders," *IEEE Transactions on Circuits and Systems for Video Technology*, vol. 34, no. 9, pp. 8779–8793, 2024.
- [28] X. Ren and J. Malik, "Learning a classification model for segmentation," in *ICCV*, vol. 2, 2003, pp. 10–10.
- [29] P. F. Felzenszwalb and D. P. Huttenlocher, "Efficient graph-based image segmentation," *IJCV*, vol. 59, no. 2, pp. 167–181, 2004.
- [30] M.-Y. Liu, O. Tuzel, S. Ramalingam, and R. Chellappa, "Entropy rate superpixel segmentation," in *CVPR*, 2011, pp. 2097–2104.
- [31] R. Achanta, A. Shaji, K. Smith, A. Lucchi, P. Fua, and S. Süssstrunk, "Slic superpixels compared to state-of-the-art superpixel methods," *TPAMI*, vol. 34, no. 11, pp. 2274–2282, 2012.
- [32] Y.-J. Liu, C.-C. Yu, M.-J. Yu, and Y. He, "Manifold slic: A fast method to compute content-sensitive superpixels," in *CVPR*, 2016, pp. 651–659.
- [33] J. Yao, M. Boben, S. Fidler, and R. Urtasun, "Real-time coarse-to-fine topologically preserving segmentation," in *Proceedings of the IEEE conference on computer vision and pattern recognition*, 2015, pp. 2947–2955.
- [34] M. Van den Bergh, X. Boix, G. Roig, and L. Van Gool, "Seeds: Superpixels extracted via energy-driven sampling," *International Journal of Computer Vision*, vol. 111, pp. 298–314, 2015.
- [35] D. Yeo, J. Son, B. Han, and J. Hee Han, "Superpixel-based tracking-by-segmentation using markov chains," in *CVPR*, 2017, pp. 1812–1821.
- [36] R. Achanta and S. Susstrunk, "Superpixels and polygons using simple non-iterative clustering," in *CVPR*, 2017, pp. 4651–4660.
- [37] F. Yang, Q. Sun, H. Jin, and Z. Zhou, "Superpixel segmentation with fully convolutional networks," in *CVPR*, 2020, pp. 13964–13973.
- [38] L. Cai, X. Xu, J. H. Liew, and C. S. Foo, "Revisiting superpixels for active learning in semantic segmentation with realistic annotation costs," in *CVPR*, 2021, pp. 10988–10997.
- [39] W.-C. Tu, M.-Y. Liu, V. Jampani, D. Sun, S.-Y. Chien, M.-H. Yang, and J. Kautz, "Learning superpixels with segmentation-aware affinity loss," in *CVPR*, 2018, pp. 568–576.
- [40] A. Zhang, W. Ren, Y. Liu, and X. Cao, "Lightweight image super-resolution with superpixel token interaction," in *Proceedings of the IEEE/CVF International Conference on Computer Vision*, 2023, pp. 12728–12737.
- [41] B. Peng, X. Jin, J. Liu, D. Li, Y. Wu, Y. Liu, S. Zhou, and Z. Zhang, "Correlation congruence for knowledge distillation," in *ICCV*, 2019.
- [42] C. Yang, H. Zhou, Z. An, X. Jiang, Y. Xu, and Q. Zhang, "Cross-image relational knowledge distillation for semantic segmentation," in *CVPR*, 2022.
- [43] Y. Liu, J. Cao, B. Li, C. Yuan, W. Hu, Y. Li, and Y. Duan, "Knowledge distillation via instance relationship graph," in *CVPR*, 2019.
- [44] A. Vaswani, N. Shazeer, N. Parmar, J. Uszkoreit, L. Jones, A. N. Gomez, L. Kaiser, and I. Polosukhin, "Attention is all you need," in *NeurIPS*, I. Guyon, U. von Luxburg, S. Bengio, H. M. Wallach, R. Fergus, S. V. N. Vishwanathan, and R. Garnett, Eds., 2017, pp. 5998–6008.
- [45] O. Russakovsky, J. Deng, H. Su, J. Krause, S. Satheesh, S. Ma, Z. Huang, A. Karpathy, A. Khosla, M. Bernstein, A. C. Berg, and L. Fei-Fei, "Imagenet large scale visual recognition challenge," *IJCV*, 2015.
- [46] K. He, X. Chen, S. Xie, Y. Li, P. Dollár, and R. Girshick, "Masked autoencoders are scalable vision learners," in *Proceedings of the IEEE/CVF conference on computer vision and pattern recognition*, 2022, pp. 16000–16009.
- [47] K. He, X. Zhang, S. Ren, and J. Sun, "Deep residual learning for image recognition," in *IEEE CVPR*, 2016.
- [48] I. Radosavovic, R. P. Kosaraju, R. Girshick, K. He, and P. Dollár, "Designing network design spaces," in *IEEE CVPR*, 2020.
- [49] M. Tan and Q. V. Le, "Efficientnet: Rethinking model scaling for convolutional neural networks," *preprint arXiv:1905.11946*, 2019.
- [50] A. Krizhevsky, G. Hinton *et al.*, "Learning multiple layers of features from tiny images," 2009.
- [51] J. Krause, M. Stark, J. Deng, and L. Fei-Fei, "3d object representations for fine-grained categorization," in *Proceedings of the IEEE international conference on computer vision workshops*, 2013, pp. 554–561.
- [52] A. Romero, N. Ballas, S. E. Kahou, A. Chassang, C. Gatta, and Y. Bengio, "Fitnets: Hints for thin deep nets," *arXiv preprint arXiv:1412.6550*, 2014.



Zhaoyi Yan received the Ph.D. degree in Computer Science from Harbin Institute of Technology, China, in 2021. His research interests include deep learning, image inpainting, crowd counting, knowledge distillation and Large Language Models. He has published more than 10 papers in conferences and journal including CVPR, ICCV, ECCV, AAAI, TNNLS and TCSVT.



Kangjun Liu received the Ph.D. degree in information and communication engineering from South China University of Technology, China, in 2023. He is a postdoctoral researcher in Peng Cheng Laboratory, Shenzhen, China. His research interests include computer vision, representation learning and pattern recognition. He has published several papers in conferences and journals including TIP and PR.



Qixiang Ye (M'10-SM'15) received the B.S. and M.S. degrees in mechanical and electrical engineering from Harbin Institute of Technology, China, in 1999 and 2001, respectively, and the Ph.D. degree from the Institute of Computing Technology, Chinese Academy of Sciences in 2006. He has been a professor with the University of Chinese Academy of Sciences since 2009, and was a visiting assistant professor with the Institute of Advanced Computer Studies (UMIACS), University of Maryland, College Park until 2013. His research interests include image processing, object detection and machine learning. He has published more than 100 papers in refereed conferences and journals including IEEE CVPR, ICCV, ECCV and TPAMI, TIP and TCSVT. He is on the editorial board of IEEE Transactions on Circuit and Systems on Video Technology.